Nordic Concrete Research – Publ. No. NCR 58 – ISSUE 1 / 2018 – Article 1, pp. 1-16

DOI: 10.2478/ncr-2018-0001

ISSN online 2545-2819

ISSN print 0800-6377

Received: March 12, 2018

Revision received: May 3, 2018

Accepted: May 3, 2018

Long-term Influence of Concrete Surface and Crack Orientation on Self-healing and Ingress in Cracks – Field Observations

Tobias Danner
MSc, PhD, Researcher
Norwegian University of Science and Technology
Department of Structural Engineering
Richard Birkelandsvei 1a, NO-7491 Trondheim
tobias.a.danner@ntnu.no

Mette Rica Geiker
MSc, PhD, Professor
Norwegian University of Science and Technology
Department of Structural Engineering
Richard Birkelandsvei 1a, NO-7491 Trondheim
mette.geiker@ntnu.no

ABSTRACT
This paper presents results from investigations on the long-term influence of concrete surface and crack orientation on ingress in cracks. Five reinforced concrete structures from Norway exposed to either de-icing salts or seawater have been investigated. Concrete cores were taken with and without cracks from surfaces with vertical and horizontal orientation. Carbonation in cracks was found on all de-iced structures, and a crack on a completely horizontal surface appeared to facilitate chloride ingress. Ingress of substances from seawater was found in all cracks from marine exposure. However, the impact of cracks on chloride ingress was unclear. Horizontal cracks on vertical surfaces appeared to facilitate self-healing.

Key words: Cracks, exposure, ingress, field observations, long-term

1. INTRODUCTION

The research presented in this paper is part of the ongoing research project “Ferry-free coastal route E39” initiated by the Norwegian Public Roads Administration. A main part of project WP 7.1.1 “Relevance of crack width and decompression requirements (limits) due to durability aspects of conventional reinforcement” is the collection of long-term field data on the influence of cracks on chloride ingress and reinforcement corrosion. Furthermore, the impact of exposure and orientation of concrete surface and cracks on self-healing and chloride ingress is investigated. This paper presents results from field studies performed in 2017.

Reinforcement corrosion due to chloride ingress or carbonation is one of the major deterioration mechanisms of steel reinforced concrete structures. There is evidence that cracks facilitate the ingress of chloride ions and shorten the time to initiate reinforcement corrosion [1].

According to Eurocode 2 [2] a limiting calculated crack width (w_{max}) should be established to maintain proper functioning or durability of reinforced concrete structures. For ordinary reinforcement and exposure classes XC, XD and XS the recommended value for w_{max} is 0.3 mm [2]. The *fib* model code for service life design (MC-SLD) [3] gives guidelines on the impact of cracks on service life. These guidelines for chloride and carbonation induced corrosion are summarized in Table 1 and Table 2. Horizontal surfaces with cracks and chloride exposure from top are regarded the most severe exposure condition. In this case special protective measures should be taken in the presence of cracks to ensure service life ≥ 10 years. For vertical or horizontal concrete surfaces with exposure from the bottom, service life ≥ 50 years is expected for surface crack width ($w_{k,cal}$) up to 0.3 mm given high quality concrete (cover ≥ 50 mm and w/c ≤ 0.5). For carbonation induced corrosion, there is no differentiation made between horizontal and vertical surfaces. The concrete should be of “adequate quality” and $w_{k,cal} \leq 0.3$ mm to obtain a service life of at least 50 years [3].

Table 1 - Crack width guidelines for chloride induced corrosion on horizontal and vertical surfaces according to MC-SLD [3].

Surface	Exposure	Crack	Crack width ($w_{k,cal}$)	Protective measure	Service life
Horizontal	From top	On top	No limit	Special measures	≥ 10 years
Horizontal Vertical	From bottom	Water not leaking through cracks	≤ 0.3 mm	High quality concrete (cover ≥ 50mm; w/c ≤ 0.5)	≥ 50 years

Table 2 - Crack width guidelines for carbonation induced corrosion according to MC-SLD (2006) [3].

Surface	Exposure	Crack	Crack width ($w_{k,cal}$)	Protective measure	Service life
-	-	-	≤ 0.3 mm	Adequate concrete cover	≥ 50 years

Laboratory experiments of the influence of cracks on chloride ingress and corrosion are mainly performed on horizontal concrete surfaces with exposure from the top. A typical experimental set up is ponding of a crack with chloride solution from top [4]. When discussing the orientation of cracks, the orientation is only described with regard to the reinforcement, *i.e.* coincident cracks (parallel to reinforcement) and intersecting cracks (perpendicular to the reinforcement); but not with regard to the concrete surface [5].

Self-healing of cracks in concrete is highly dependent on the exposure condition and the presence of water is the most important factor [6]. The main mechanisms of self-healing seem to be of chemical nature. Chemical causes of self-healing of cracks exposed to water are *e.g.* further hydration of unhydrated cement grains or the formation of calcium carbonate crystals on the crack surface. The formation of calcium carbonate on crack surfaces is examined in detail and considered the most important mechanism of autogenic self-healing in the presence of fresh water [7]. Formation of C-S-H phases, portlandite and ettringite was observed in cracks after 3 month curing in water [8]. For cracked concrete exposed to seawater the formation of brucite ($Mg(OH)_2$) or ettringite was also observed [9-11].

Only very few studies investigated the impact of surface and/or crack orientation on ingress. Most studies do not describe the exposure conditions in detail. Information on the surface orientation is typically lacking. According to the authors' knowledge there are no data available on the impact of crack and surface orientation on self-healing of cracks. This paper presents observations from field studies on chloride ingress and self-healing in cracks with regard to surface orientation and crack orientation.

2. MATERIALS AND METHODS

2.1 Materials

Investigated Structures

Table 3 gives an overview of the investigated field structures. Figure 1 shows the location of the investigated field structures. The investigations covered three structures exposed to de-icing salts (Cecilie Bridge, Tåsen Tunnel and Moholt Bridge) and two marine exposed structures (DNV column and Hafrsfjord Bridge). The investigations on Cecilie (16 years old) and Moholt Bridge (25 years old) concentrated on shrinkage cracks in the edge beams. The exact exposure of the edge beams is not well documented. The investigated edge beams were adjacent to the pedestrian path which was not salted. However, the driving lane was regularly salted as part of winter maintenance. Salt could have been transported to the edge beams by wind and salt spray due to frequent traffic. Additionally, the bridges are only 1 and 2 kilometres away from Trondheim fjord which could lead to some airborne chloride exposure. Similarly, it was not possible to define the exact exposure of the concrete core received from Tåsen Tunnel (20 years old). Inside the tunnel, no de-icing salts are used. However, the road where the tunnel is located is categorized in the highest priority class of winter maintenance in Norway, meaning regular use of de-icing salts. The distance between tunnel drive in and the location of the core was about 1 km. Both the DNV column and the foundations of Hafrsfjord Bridge are exposed to tidal seawater for 33 and 50 years, respectively. The DNV column was reinforced with three concentric reinforcement cages, parts of which was coupled to a sacrificial anode for an unknown period [12]. It is our expectation that the impact on ingress has been limited due to a very low current, as no corrosion of the reinforcement cages was observed after removing all the concrete.

Figure 2 illustrates the investigated structural parts showing the different orientation of the investigated concrete surfaces and the orientation of the investigated cracks. The red circles indicate locations of coring. Concrete cores were taken from horizontal and vertical surfaces. The edge beam from Cecilie Bridge was the only completely horizontal surface of all investigated structural parts. The edge beam from Moholt Bridge had a slope of about 4 %. From Tåsen Tunnel, the DNV column and the foundation of Hafrsfjord Bridge, cores were taken on vertical surfaces.

Table 3 - Overview over investigated structures [13]

Structure	Cecilie Bridge	Tåsen Tunnel	Moholt Bridge	DNV column	Hafrsfjord Bridge
Type	Beam (Box-girder) bridge	Culvert	Slab bridge	Part time dynamically loaded column	Beam bridge (NIB)
Location	Trondheim	Oslo	Trondheim	Bergen	Stavanger
Structural part	Edge beam	Tunnel wall	Edge beam	Column	Foundation
Cracks	Shrinkage	Shrinkage	Shrinkage	Dynamic loading	Shrinkage, restraint
Cover (mm)	70	50	50	50	90
Concrete	C55	N/A *	C45	C60	B35
Cement	N/A	N/A	N/A	SP 30-4A	N/A
Cement Type	N/A	N/A	N/A	CEM I	N/A
Surface orientation	Horizontal	Vertical	Horizontal	Vertical	Vertical
Crack orientation	Vertical	Vertical	Vertical	Horizontal	Vertical
Age (years)	16	20	25	33	50
Exposure	De-icing salt	De-icing salt	De-icing salt	Tidal seawater	Tidal seawater
Climate	Inland	Inland	Inland	Marine	Marine

* N/A: not available

Figure 1 – Map of Norway showing the location of the investigated bridges, after [14]

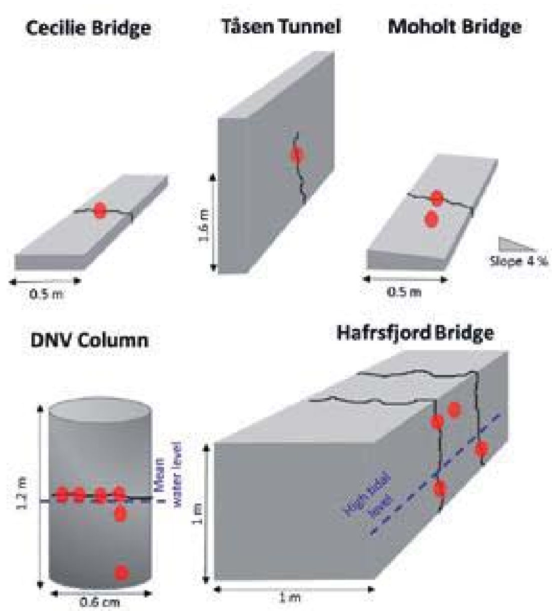

Figure 2 - Illustration of the investigated structural parts showing the concrete surface and crack orientation. Locations were cores where taken are illustrated in red.

While the Tåsen Tunnel and Hafrsfjord Bridge had vertical cracks, the DNV column had a crack with horizontal orientation. Except for the DNV column, it is expected that the investigated cracks are due to early drying shrinkage or thermal restraint. The investigated crack from the DNV column derives from dynamic loading [15]. None of the structures allowed cores to be taken from different surfaces or crack orientations.

Concrete Cores
For all structures it was tried to drill concrete cores through reinforcement with crack width above and below 0.3 mm [2]. Additionally, reference cores next to the cracks were taken when possible. Table 4 gives an overview of the drilled concrete cores from the investigated field structures. The approximate location of concrete cores is illustrated in Figure 2.

For Cecilie Bridge and Tåsen Tunnel it was only possible to retrieve one (1) core for the investigation. The concrete cores from both structures were drilled on a surface crack with crack width 0.45 mm. Three (3) cores were drilled from Moholt Bridge, with no crack and surface crack widths of 0.2 and 0.55 mm. The crack mouth of the investigated cracks from the de-iced structures appeared open.

From the DNV column six (6) concrete cores were drilled. Four (4) concrete cores were drilled on the horizontal crack in the tidal zone. Two (2) reference cores were drilled below the crack in the tidal zone. Core D_0aT was drilled only about 0.1 m below the crack while core D_0bT was drilled about 0.4 m below the crack. The crack was located close to the mean water level. The location of the mean water level at the DNV column is illustrated in Figure 2. The tidal changes in Bergen at the field station are about ± 0.8 m. The surface crack width on the cores varied between 0.15 to 0.50 mm. [16]

Six (6) concrete cores were taken from Hafrsfjord Bridge. Four (4) cores including a reference without crack were taken from the tidal zone. The mouth of the cracks in the tidal zone appeared sealed. The surface crack width was about 0.20 mm. Two (2) cores with cracks were taken in the splash zone. The surface crack width of these cores was 0.40 and 0.50 mm and the crack mouth appeared open.

Table 4 - Overview of the concrete cores taken from the different structures

Structure	Core id.	Exposure	Height above mean water level (m)	Surface crack width (mm)	Crack depth (mm)	Concrete cover (mm)	Crack mouth open/sealed
Cecilie Bridge	C_0.45D*	De-iced		0.45	70 (wc)**	70	Open
Tåsen Tunnel	*T_0.45D*	De-iced		0.45	50 (wc)	50	Open
Moholt	M_0D	De-iced		0.00		50	
Bridge	M_0.2D	De-iced		0.20	40		Open
	M_0.55D	De-iced		0.55	70 (wc)		Open
DNV	*D_0aT**	Tidal	-0.1	0.00		50	
column	*D_0bT*	Tidal	-0.4	0.00	150 (wc)		
	D_0.2aT	Tidal	+0.1	0.20	150 (wc)		Sealed
	D_0.5T	Tidal	+0.1	0.50	150 (wc)		Sealed
	D_0.15T	Tidal	+0.1	0.15	150 (wc)		Sealed
	D_0.2bT	Tidal	+0.1	0.20	150 (wc)		Sealed
Hafrsfjord	*H_0T*	Tidal	0	0.00		90	
Bridge	H_0.2aT	Tidal	0	0.20	100 (wc)		Sealed
	H_0.2bT	Tidal	0	0.20	110 (wc)		Sealed
	H_0.2cT	Tidal	0	0.20	120 (wc)		Sealed
	*H_0.4S**	Splash	+0.6	0.40	120 (wc)		Open
	H_0.5S	Splash	+0.6	0.50	110 (wc)		Open

* D: de-icing salts; T: tidal zone; S: splash zone
** wc : whole core
Italic = extracted with reinforcement

2.2 Methods

Surface crack width measurements were performed manually with a crack width ruler (accuracy ± 0.05 mm) on the concrete surface before drilling of the concrete cores. The measurements were undertaken during spring or autumn at temperatures between 5 and 15°C.

Concrete cores were drilled with a water-cooled concrete saw and tapped dry. After a fast visual inspection in the field, the cores were tightly packed in several layers of plastic. Before analysis and in between experiments, the cores were stored in plastic in a room with a temperature of 5°C.

The concrete cores were used for chloride profile grinding and μ-XRF elemental mapping. The concrete cores were cut into two halves with a water-cooled concrete saw and tapped dry with a moist cloth. Quantitative chloride profiles were taken from one of the halves of concrete cores not containing cracks. Profile grinding was done in 5 mm steps for the first 30 mm and 10 mm steps from 30-100 mm. Thin layers were ground inwards from the exposed surface. The chloride content of these layers was determined with potentiometric titration method. About 5 g of the concrete powder of each section was dissolved in 50 ml 80°C (1:19) HNO_3 and filtrated after 1 h. The chloride content in the resulting filtrated solution was determined by potentiometric titration with a Titrando 905 titrator from Metrohm. 0.01 M $AgNO_3$ was used as titrant. [17]

Concrete cores taken with and without cracks were analysed with micro X-Ray fluorescence (μ-XRF) without further preparation [18] Elemental maps were obtained on a M4 Tornado from Bruker. The instrument operates with a Ag X-Ray source and two silicon drift detectors simultaneously for fast analysis. A collimator focuses the X-ray beam to a spot size of about 25 μm. Elemental maps were acquired with 50 kV accelerating voltage and 600 μA tube current. A distance of 60 μm between each measuring point and a speed of 1 ms/pixel were chosen for qualitative maps. For each map, the signal detected as counts per second (cps) is normalized to 100 %. The brightest areas represent the highest measured cps. All maps are normalized individually and colour codes should not be compared directly.

Carbonation depth was characterized by spraying the freshly cut concrete surface with thymolphthalein indicator. After cutting, the concrete surface was dried with paper prior to spraying with the indicator solution. The thymolphthalein solution was prepared by dissolving 1 g of the indicator (powder, grade “ACS, Reag. Ph Eur” (VWR)) in a mix of 30 ml of deionized water and 70 ml of ethanol [19]. Thymolphthalein gives a colour change in the pH range of 9 to 10.5 Above this range, the colour of thymolphthalein gets bluish while, below it, thymolphthalein becomes colourless.

3. RESULTS AND DISCUSSION

In the results and discussion chapter the expression “self-healing of cracks” will be used in cases where a precipitation of new phases was observed inside the crack. However, neither mechanical nor ingress tests were performed to verify if the investigated cracks actually were self-healed or self-sealed, respectively.

3.1 De-iced Structures

Figure 3 shows the μ-XRF chlorine maps of concrete cores taken from Cecilie Bridge, Tåsen Tunnel and Moholt Bridge. The surface crack width of the cracks was 0.45 mm for Cecilie Bridge and Tåsen Tunnel and 0.55 mm for Moholt Bridge. Figure 3 (left) shows the chloride ingress in the cracked concrete core from Cecilie Bridge. An even chloride ingress over the whole width of the concrete core is visible within the first 10 mm. Besides that, chloride ingress is visible along the crack. Chloride ingress from the crack surface into the concrete was observed over the full length of the core, i.e. 100 mm. In contrast to this, the concrete cores from Tåsen Tunnel (Figure 3 middle) and Moholt Bridge (Figure 3 right) did not show an impact of the crack on the chloride ingress.

In the core from Tåsen Tunnel, somewhat higher chlorine intensities were observed around the steel-concrete interface compared to the bulk of the concrete. A possible explanation could be micro-cracking in the steel-concrete interface facilitating the accumulation of chloride. The surface crack width was similar in the core from Cecilie Bridge and Tåsen Tunnel. However, the core from Cecilie Bridge was taken from a horizontal surface, while a crack from a vertical surface was investigated in Tåsen Tunnel. The time of direct exposure is generally longer on a horizontal surface, which can explain the higher ingress into the crack observed in Cecilie Bridge.

In the core from the Moholt Bridge, there seems to be a very low level of chloride ingress in the concrete surface. The measured intensities in the surface near region are not much higher than in the bulk of the concrete i.e. almost disappearing in the background noise. The investigated edge beam from Moholt Bridge is similar to the edge beam investigated on Cecilie Bridge, except for the slope. Both bridges are categorized in the same winter maintenance class and the wind exposure is similar. However, compared to Cecilie Bridge the edge beam of Moholt Bridge is not completely horizontal but had a slope of 4%.

In cores drilled above reinforcement from Moholt Bridge and Tåsen Tunnel general corrosion was found on the surface of the steel in contact with carbonated concrete. However, the extent of corrosion was limited. Carbonation in cracks was observed in all cores taken from de-iced structures regardless of the surface crack width. Figure 4 shows the corrosion imprint in the steel-concrete interface, general corrosion on the reinforcement and the carbonation of the crack surface from the concrete core taken from Moholt Bridge. The example shown is from the concrete core with limited chloride ingress presented in Figure 3 (right).

Figure 3 - µ-XRF chlorine maps of concrete cores from de-iced structures. Left: Core C_0.45D from the Cecilie Bridge; Middle: Core T_0.45D from the Tåsen Tunnel; Right: Core M_0.55D from the Moholt Bridge. The orientation of the cores represents the surface orientation in the field. R = reinforcement

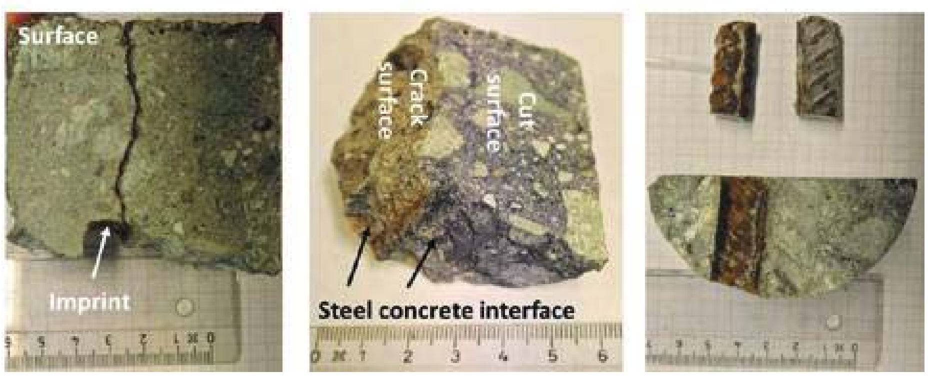

Figure 4 - Concrete core M_0.55D from the Moholt Bridge. Left: Cut concrete core; Middle: Carbonated crack surface and steel-concrete interface of the corroded rebar Right: General corrosion on the upper surface of the reinforcement and corrosion imprint in the steel-concrete interface for the reinforcement beneath the crack.

3.2 Marine Structures

For the marine exposed structures, quantitative chloride profiles of reference cores without crack were taken. µ-XRF mapping was performed on concrete cores with and without cracks. Figure 5 shows the chloride profiles of a core from the 33-year-old DNV column (D_0aT) and the 50-year-old Hafrsfjord Bridge (H_0T). The chloride profiles look similar with about 0.6 % Cl by weight of concrete in the outer 10 mm of the concrete cores.

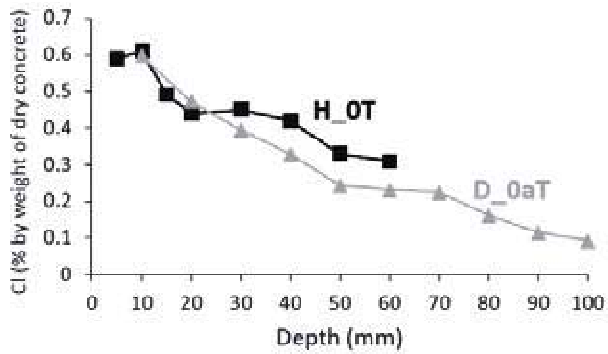

Figure 5 - Quantitative chloride profiles of cores H_0T and D_0aT from Hafrsfjord Bridge and the DNV column, respectively. Both cores were without crack and from the tidal zone.

Figure 6 shows the chlorine, magnesium and sulphur maps of four concrete cores from the DNV column. The first core to the left is the reference core with no crack. All four concrete cores show an even chloride ingress from the concrete surfaces. Compared to the reference core there is no apparent deeper chloride ingress in the cracked cores. In the crack of core D_0.5T, magnesium is visible within the first 20 mm. In cores D_0.15T and D_0.2T, the cracks are difficult to see due their small size and the extensive self-healing observed in these cracks. Magnesium and calcium rich products were found in all cracks, which is typical for self-healing of concrete exposed to seawater [9, 11]. Right after cutting and after cleaning the reinforcement with acid, no corrosion was observed. During storage, corrosion developed on the cut steel surfaces in the concrete cores. Corrosion was especially observed on the outer reinforcement, which can be explained by a higher chloride content in this area. Further details on the investigations performed on the DNV column are given in [14].

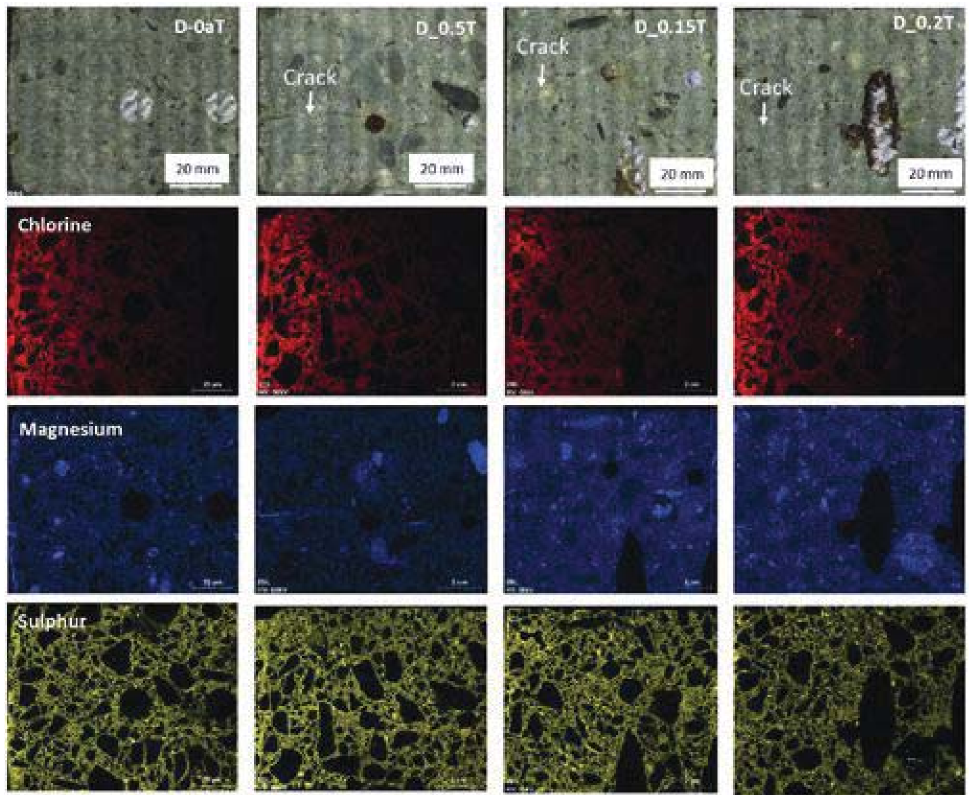

Figure 6 - Chlorine, magnesium and sulphur maps from cores from the DNV column. ***Left:*** *Core D_0aT without crack from the tidal zone;* ***Middle left:*** *Core D_0.5T, surface crack width 0.5 mm;* ***Middle right:*** *Core D_0.15, surface crack width 0.15 mm;* ***Right:*** *Core D_0.2, surface crack width 0.2 mm. The cracked concrete cores were located about 0.2 m higher than the reference concrete core without crack. The indicated cracks are partly healed.*

Figure 7 shows the chlorine, magnesium and sulphur maps of four concrete cores from Hafrsfjord Bridge from the tidal and splash zone. The first core to the left is the reference core with no crack. In the field, it was observed that the crack mouth was sealed in the tidal zone. The same cracks but higher up (splash zone) had an open crack mouth. When the concrete cores were extracted, the crack surfaces did not show signs of self-healing, independently of exposure. Most cores fell apart along the crack surface and had to be taped together for µ-XRF analysis. The cracks of the concrete cores shown in Figure 7 appear therefore larger than the original size. The sealing of the crack mouths in the tidal zone might be explained by leaching from the cement paste followed by precipitation. Although, no self-healing was observed, magnesium precipitation on the crack surfaces was detected with µ-XRF in all cores. Furthermore, ingress of sulphate through the cracks is clearly visible from the sulphate maps. While magnesium seems to precipitate on the crack surfaces, sulphur appears to diffuse into the concrete. Magnesium and sulphate were detected as deep as 100 mm in core H_0.4S. The very light spots in the sulphur maps are pores, and are also visible in the calcium mapping. This could be explained by potential precipitation of gypsum on the pore walls. Despite, the clear ingress of seawater in to the cracks, an impact of the cracks on chloride ingress was not detectable.

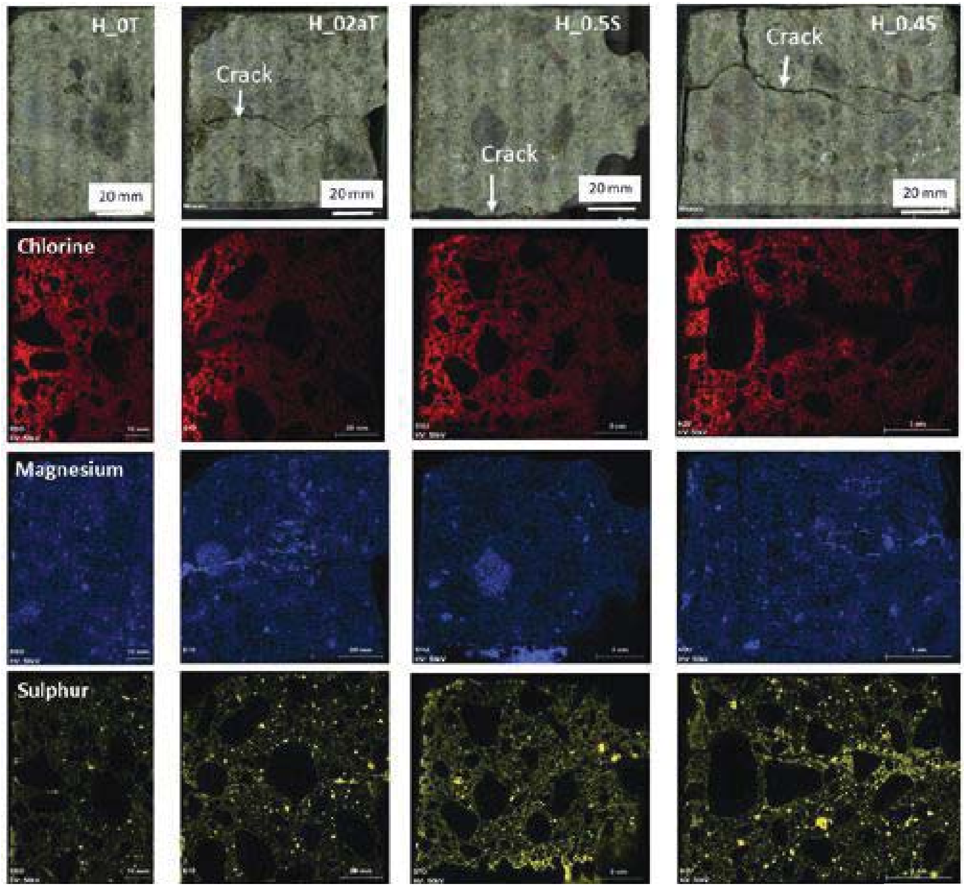

Figure 7 - Chlorine, magnesium and sulphur maps from cores from the Hafrsfjord Bridge. ***Left:*** *Core H_0T without crack from the tidal zone;* ***Middle left:*** *Core H_0.2aT, surface crack width 0.2 mm, from the tidal zone at the same height as core H_0T;* ***Middle right:*** *Core H_0.5S, surface crack width 0.5 mm from the splash zone;* ***Right:*** *Core H_0.4S, surface crack width 0.4 mm, from the splash zone.*

Two cores from Hafrsfjord Bridge (H_0T and H_0.5S) were drilled through reinforcement, one off crack and one on crack. Both the uncracked reference core (H_0T) and the cracked core (H_0.5S) did not show signs of reinforcement corrosion. Compared to the other investigated structures, the cover depth at the foundations of Hafrsfjord Bridge was higher with about 90 mm.

As mentioned before, magnesium precipitation was observed inside cracks for both, the DNV column and Hafrsfjord Bridge. However, self-healing was only observed in cores taken from the DNV column. Figure 8 shows a close up picture of the crack in core H_0.2aT from Hafrsfjord Bridge and core D_0.5T from the DNV column. In core H_0.2aT we can see an open crack with some precipitation on the crack surface. In core D_0.5T we can see a layer of products closing the crack. In both cases, the phases were rich in calcium and magnesium.

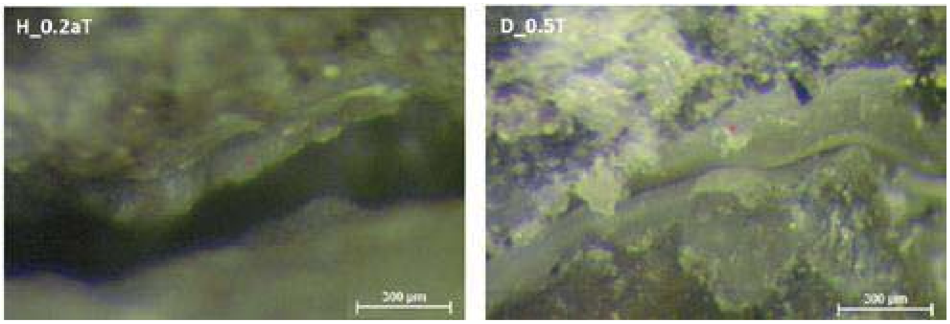

Figure 8 - Left: Open, not self-healed crack of core H_0.2aT from the Hafrsfjord Bridge; Right: Closed, self-healed crack of core D_0.5T from the DNV column.

3.3 Influence of concrete surface and crack orientation on ingress and self-healing

Table 5 gives a summary of the obtained results with regard to chloride ingress, carbonation, self-healing and corrosion.

Table 5 - Summary of results on chloride ingress and carbonation along cracks and self-healing of the analysed concrete cores from the different structures.

Structure	Concrete surface	Surface crack width (mm)	Crack orientation	Impact of crack on chloride ingress	Carbonation in cracks	Self-healing	Impact of crack on corrosion
Cecilie Bridge	Horiz.	0.45	Vertical	Yes	Yes	No	N/A
Tåsen Tunnel	Vert.	0.45	Vertical	No	Yes	No	N/A
Moholt	Horiz.	0.0	Vertical				
Bridge		0.2		No	Yes	No	
		0.45		No	Yes	No	Yes
DNV Field	Vert.	0.0	Horizontal				No - CP
Station		0.2		No	No	Yes	No - CP
		0.5		No	No	Yes	No - CP
Hafrsfjord	Vert.	0.0	vertical				
Bridge		0.2		No	No	No	N/A
		0.45		No	No	No	No

N/A = not available
CP = potentially cathodic protected via sacrificial anodes

Carbonation of cracks was observed on all the de-iced structures regardless of the surface orientation, and carbonation induced corrosion was observed on the reinforcement surface extracted with cores from the de-iced structures. A clear impact of a crack on chloride ingress was only observed for the completely horizontal surface (Cecilie Bridge).

Ingress of seawater in the cracks was observed in magnesium and sulphur mappings; however, a potential impact of cracks on chloride ingress was not detectable. The horizontal crack on the marine exposed DNV column seem to favour self-healing, and complete self-healing of cracks was only observed in the cores taken from the DNV column. In contrast, the vertical crack on the Hafrsfjord Bridge was not self-healed. This might be explained by a horizontal crack being wet for longer time, as seawater might stay longer inside the crack after it is filled. In a vertical crack the water can move more freely out of the crack.

Figure 9 illustrates the observed long-term influence of concrete surface and crack orientation on ingress in cracks. A crack on a horizontal top surface (1) appears to represent the most severe condition with regard to ingress. This supports the guidelines given in the *fib* model code for service life design (MC-SLD) [3]. A crack on a vertical surface is less severe. The potential for self-healing of a crack in marine exposure seems to be facilitated with a horizontal crack, i.e. vertical cracks (2) appears more severe than horizontal cracks (3).

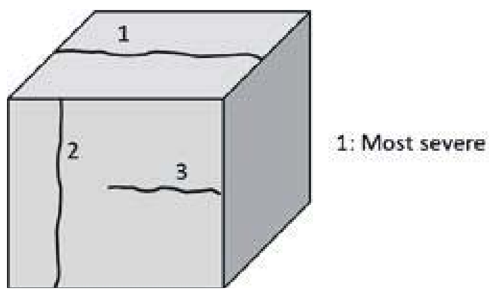

Figure 9 - Illustration of the observed long-term influence of concrete surface and crack orientation on ingress in cracks.

4. CONCLUSIONS

This research presents preliminary results from a limited amount of samples. However, there are some indications on the influence of exposure and orientation of surface and cracks on ingress and self-healing as listed below.

- On de-iced structures, chloride ingress in cracks was only observed on a completely horizontal surface. This supports the guidelines in MC-SLD describing horizontal surfaces with exposure from top as the most severe condition [3].
- Complete carbonation of crack surfaces was observed on all three structures exposed to de-icing salts regardless of surface crack width and surface orientation.
- On the two marine exposed structures, ingress of magnesium and sulphur from seawater was observed. Magnesium was precipitated inside the crack, while sulphur diffused from the crack surfaces into the concrete. The impact of cracks on chloride ingress was unclear.
- Complete self-healing of cracks was only observed for a horizontal crack on a vertical surface exposed to the marine tidal zone.

ACKNOWLEDGEMENTS

This research is part of the Norwegian Public Roads Administration (NPRA) Ferry-free coastal route project. NPRA and Trondheim municipality are acknowledged for providing access to Cecile-, Moholt-, Hafrsfjord Bridge and Tåsen Tunnel. DNV GL is acknowledged for providing concrete columns and NPRA is acknowledged for facilitating the collaboration. The financial sponsors of the project "Reinforcement Corrosion in Marine Concrete Structures Under Dynamic Loading" are acknowledged; the project made it possible to construct and expose the "DNV column".

REFERENCES

1. Bertolini, L., B. Elsener, P. Pedeferri, and R. Polder: "Corrosion of Steel in Concrete - Prevention, Diagnosis, Repair," Wiley-VCH, Weinheim, Germany, 2004.
2. European Committee for Standardization (CEN): "EN 1992-1-1: Eurokode 2: Design of concrete structures – Part 1-1: General Ruleas and Rules for Buildings," Brussels, Belgium 2004.
3. Fédération International du Béton (*fib*) : "Model Code for Service Life Design," *Bulletin* 34, Lausanne, Switzerland, 2006.
4. Michel, A., A.O.S. Solgaard, B.J. Pease, M.R. Geiker, H. Stang, and J.F. Olsen: "Experimental Investigation of the Relation between Damage at the Concrete-Steel Interface and Initiation of Reinforcement Corrosion in Plain and Fibre Reinforced Concrete," *Cement and Concrete Research*, Vol. 77, December 2013, pp. 308-321.
5. The Concrete Society: "Relevance of Cracking in Concrete to Reinforcement Corrosion," *Technical report* 44, 2nd edition. Hampshire, United Kingdom, December 2015.
6. De Rooij, M., K. Van Tittelboom, N. De Belie, and E. Schlangen: "Self healing Phenomena in Cement-based Materials," *Rilem State of the Art Report*, Rilem Technical Commitee 221-SHC, Springer, Heidelberg, Germany, 2013.
7. Edvardsen, C.: "Water Permeability and Autogenous Healing of Cracks in Concrete," *Materials Journal*.,Vol. 96(4), January 1999, pp. 448-454.
8. Jacobsen, S., J. Marchand, and H. Hornain: "Sem Observations of the Microstructure of Frost Deteriorated and Self-healed Concretes," *Cement and Concrete Research*, Vol. 25(8), December 1995, pp. 1781-1790.
9. De Weerdt, K., H. Justnes, and M.R. Geiker: "Changes in the Phase Assemblage of Concrete Exposed to Sea Water," *Cement and Concrete Composites*, Vol. 47 (Supplement C), March 2014, pp. 53-63.
10. Fidjestøl, P. and N. Nilsen: "Field Test of Reinforcement Corrosion in Concrete, in Performance of Concrete in Marine Environment," *SP-65*, American Concrete Institute, Detroit, United States of America, August 1980, pp.205-222.
11. Mohammed, T.U., N. Otsuki, and H. Hamada: "Corrosion of Steel Bars in Cracked Concrete under Marine Environment," *Journal of Materials in Civil Engineering*, Vol. 15(5), October 2003, pp. 460-469.
12. Espelid, B., A. Kyte, S.O. Valdersnes, and E. Handal: "Reinforcement Corrosion in Marine Concrete Structures under Dynamic Loading," Det Norske Veritas, Bergen, Norway, 1987.
13. Norwegian Public Roads Administration: "Brutus - Bridge and Tunnel Archive", Version 4.5.3, Oslo, Norway, March 2017.
14. www.railpass.com/plan-your-trip/maps/norway, assessed in April 2018

15. Andersen, J.H. and B. Espelid, Erfaringer fra FOU-Prosjektet "Dynamisk Belastning av Betongkonstruksjoner" in NIF-kurs: 34419020 Konstruksjoner i Lettbetong - Prosjektering og Produksjon, Det Norske Veritas, Storefjell, Norway 1993 (In Norwegian).
16. Danner, T. and M.R. Geiker: "Self-healing and Chloride Ingress in Cracked Concrete Exposed to Marine Environment for 33 Years", paper in preparation, NTNU, Trondheim, Norway, May 2018.
17. Nordtest – Nordic Innovation Centre, NT Build 443; Concrete, hardened: Accelerated Chloride Penetration, Oslo, Norway, November 1995.
18. Danner, T., De Weerdt, K.,Geiker, M.R.: "µ-XRF Charactarisation of Chloride Ingress and Self-healing in Cracked Concrete", *Proceedings*, XXIIIth Symposium on Nordic Concrete Research & Development, Aalborg, Denmark, August 2017, pp. 119-122
19. Belda Revert, A., K. De Weerdt, K. Hornbostel, and M.R. Geiker: "Carbonation-induced Corrosion: Investigation of the Corrosion Onset," *Construction and Building Materials*, Vol. 162, February 2018, pp. 847-856.